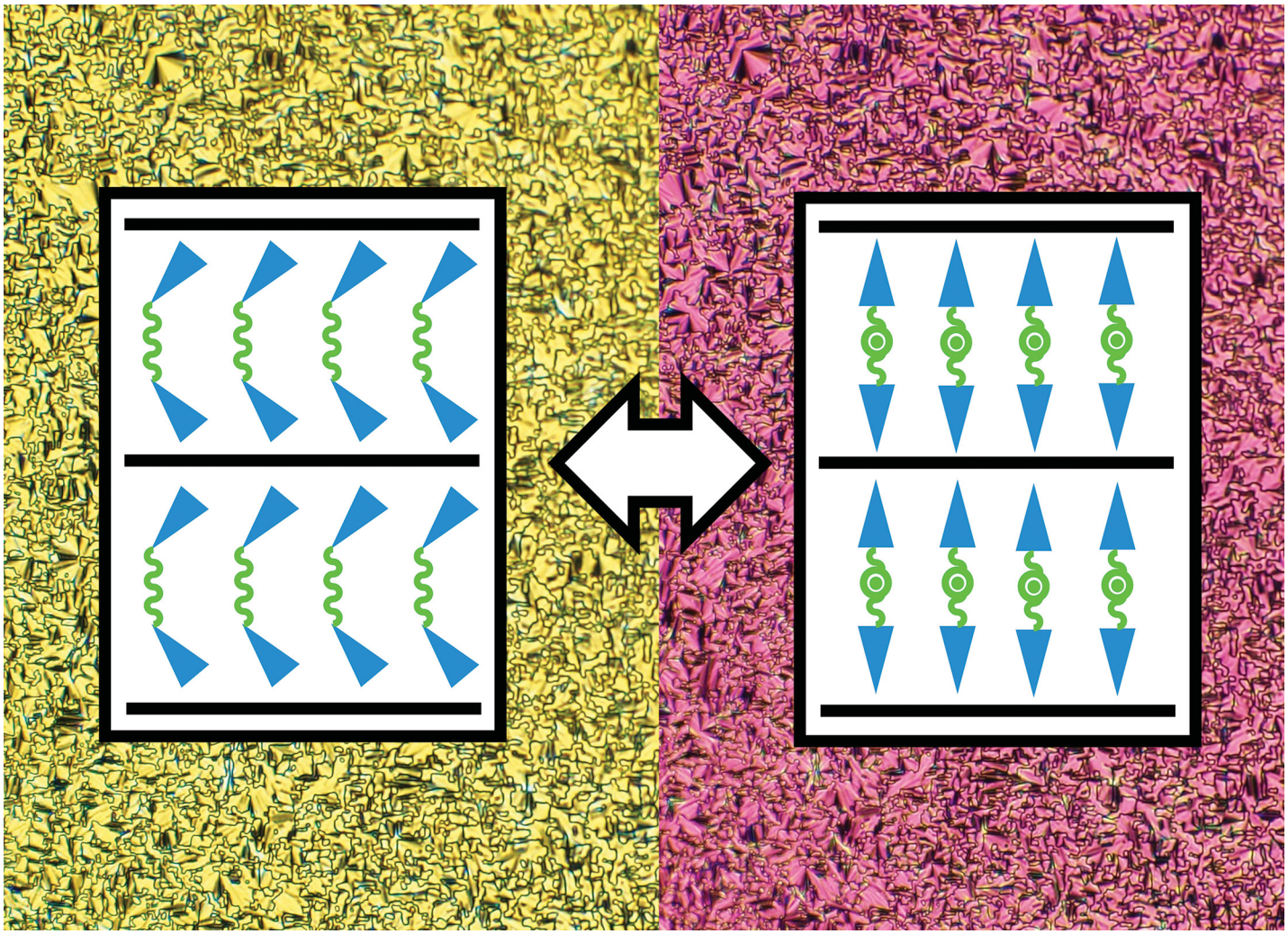

Showcasing research from Advanced Technology Research Dep., LG Japan Lab Inc., Tokyo, Japan.

Huge dielectric constants of the ferroelectric smectic-A phase in bent-shaped dimeric molecules

In the image on the left, well-developed fan-shaped textures of the $SmAP_F$ phase is observed, indicating the homogeneous alignment of the molecules, in other words, the alignment of the smectic layers perpendicular to the cell's surface. The image on the right indicates the texture under the DC bias fields. The texture does not change at all, but the birefringence color changes. This indicates that the bent (polar) direction of the molecules that are initially parallel to the cell's surface become perpendicular to it because of the ferroelectric response.

As featured in:

See Shigemasa Nakasugi *et al.*, *Mater. Adv.*, 2021, **2**, 7017.

ROYAL SOCIETY OF CHEMISTRY

rsc.li/materials-advances

Registered charity number: 207890

Materials Advances

ROYAL SOCIETY OF CHEMISTRY

PAPER

View Article Online
View Journal | View Issue

Cite this: *Mater. Adv.*, 2021, 2, 7017

Huge dielectric constants of the ferroelectric smectic-A phase in bent-shaped dimeric molecules†

Shigemasa Nakasugi, *[a] Sungmin Kang,[ab] Junji Watanabe,[b] Hiroki Ishizaki[ab] and Masato Sone[b]

Received 8th January 2021,
Accepted 8th September 2021

DOI: 10.1039/d1ma00015b

rsc.li/materials-advances

We present the dielectric relaxation properties of the ferroelectric smectic-A ($SmAP_F$) phase formed by a mixture of bent-shaped dimeric molecules α,ω-bis(4-alkoxyanilinebenzylidene-4′-carbonyloxy)pentanes with different alkyl chain lengths. The $SmAP_F$ phase shows a Goldstone-like mode at approximately 500 Hz, which can be attributed to the ferroelectricity and huge dielectric strength ($\Delta\varepsilon$). $\Delta\varepsilon$ varies dramatically with the cell thickness; in particular, it attains more than 7000 in a 50 μm-thick cell, which is much higher compared to that reported in the bent-shaped molecules.

Introduction

Since the reports on bent-shaped molecules with unique polarity by Watanabe *et al.*,[1–3] bent-shaped molecules have become an important field in the investigation of liquid crystals. In particular, the ferroelectric and the antiferroelectric smectic phases that comprise bent-shaped molecules are of great interest because they can be switched between different polar ordered states by electric fields.[2] Various bent-shaped molecules, with ferroelectric and antiferroelectric behaviors, have been synthesized and investigated to clarify the structure–property relationships associated with their profound mesomorphic properties.[4,5]

Bent-shaped dimeric molecules with two aromatic mesogens linked by an odd-carbon numbered alkyl spacer are another type of bent-shaped dimeric molecules that form polar phases.[6–9] Two mesogens in a molecule are forced to be relatively tilted to each other by the conformational constraint of the alkyl spacer.[3,10] The typical molecules are α,ω-bis(4-alkoxyanilinebenzylidene-4′-carbonyloxy)pentanes (mOAM5AMOm)[7–9] with the formula shown in Fig. 1. These bent-shaped dimeric molecules form three types of smectic liquid crystals (refer to Fig. S1, ESI†), depending on the alkoxy tail group.[7] When the tail length was short (m = 4 and 6), the $SmCA^s$ phase was formed. Here each mesogen, but not a bent-shaped dimeric molecule, participated to form each smectic layer. When the tail length was medium (m = 8–12), the frustrated $SmCA^f$ phase was formed. When the tail length was long (m = 14–18), the smectic structure was identified as the antiferroelectric SmC_AP_A phase, where each bent-shaped dimeric molecule participates in each layer comprising a bilayer of mesogenic groups. Within a layer, the bent-shaped dimeric molecules are packed with significant tilting of the molecular axis and with the same direction of the bent (polar) axis. The polar directions are opposite between the neighboring layers. Furthermore, the mixture of 4OAM5AMO4 forming the $SmCA^s$ phase and 16OAM5AMO16 forming the SmC_AP_A phase with antiferroelectricity formed the ferroelectric smectic-A ($SmAP_F$) phase in a specific ratio. The ferroelectricity of the $SmAP_F$ phase was identified by a single current peak under a triangular wave field (refer to Fig. S2, ESI†) and clear second harmonic generation.[9]

The $SmAP_F$ phase generally shows that the molecules lie perpendicular to the layer, with ferroelectric alignment of the polar directions (refer to Fig. S1(d), ESI†). Bent-shaped dimeric molecules and general bent-shaped molecules form $SmCP_F$ and $SmCP_A$, but the $SmAP_F$ phase is not commonly observed in these systems.[2,5–8] For example, W586 consisting of a bent-shaped molecule with a carbosilane group at a terminal chain suppresses out-of-layer fluctuations, favoring anticlinic tail orientation and thus the $SmAP_F$ phase due to the influence of carbosilane.[11–13] In bent-shaped dimeric molecules, mixing of 4OAM5AMO4 and 16OAM5AMO16 with different alkyl chain lengths obviously prevents the tilted association of molecules, although the reason is not clear.[9] As one of the properties of the $SmAP_F$ phase with a bent-shaped molecule, Guo *et al.* reported that W586 has high dielectric constants.[14]

In this study, we examined the dielectric relaxation properties of the $SmAP_F$ phase in bent-shaped dimeric molecules and showed extremely large dielectric constants of 2000–7000 attributable to the collective fluctuation of the polar molecules.

[a] *Advanced Technology Research Department, LG Japan Lab Inc., Shinagawa, Tokyo 140-0002, Japan. E-mail: shigemasa.nakasugi@lgjlab.com*
[b] *Institute of Innovative Research, Tokyo Institute of Technology, Yokohama, Kanagawa 226-8503, Japan*

† Electronic supplementary information (ESI) available. See DOI: 10.1039/d1ma00015b

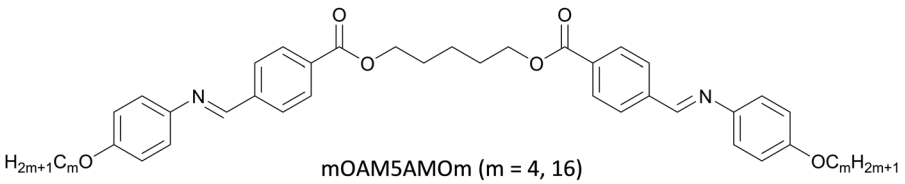

m = 4
Crystal – 89.7°C – SmCA^s – 142.5°C – Isotropic
m = 16
Crystal – 109.2°C – SmC$_A$P$_A$ – 120.0°C – Isotropic
m = 4 (65 mol%) + 16 (35 mol%)
Crystal – 89.0°C – SmAP$_A$ – 94.0°C – SmAP$_F$ – 115.0°C – Isotropic

Fig. 1 Molecular structures and phases sequence for mOAM5AMOm (m = 4, 16, and 4 + 16). The transition temperatures are taken from the DSC cooling run and the switching current curve.[9]

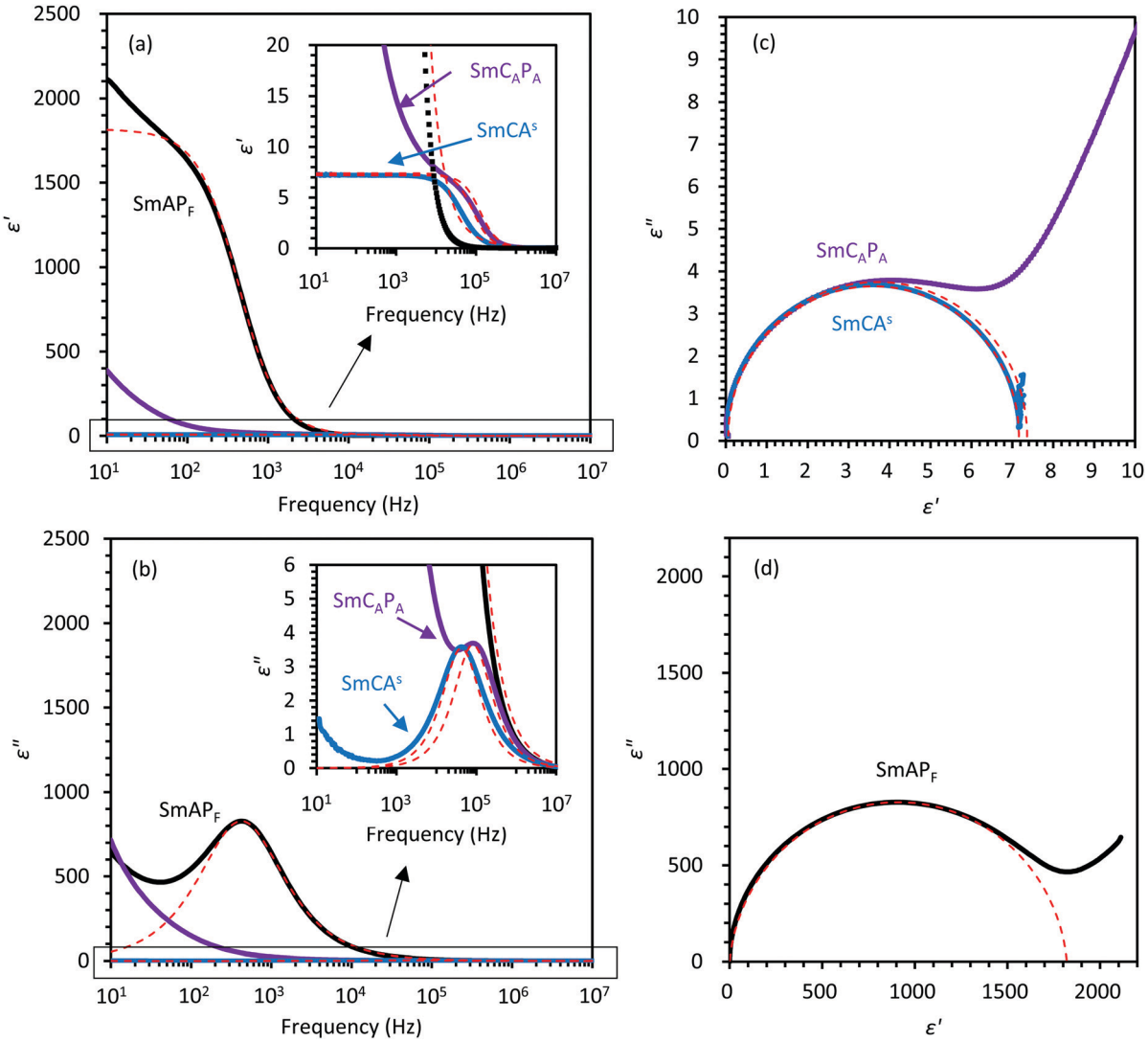

Fig. 2 (a) and (b) Frequency dependence of the real (ε') and imaginary (ε'') parts of the complex dielectric constants of the SmC$_A$P$_A$ (at 114 °C), SmCA^s (at 90 °C) and SmAP$_F$ (at 98 °C) phases, measured in a 3 μm-thick cell. In the insets, the vertical axis is expanded to clarify the high frequency mode. The dashed curves are obtained by fitting eqn (1). (c) Cole–Cole plot for the high frequency mode of the SmC$_A$P$_A$ and SmCA^s phases, and (d) Cole–Cole plot for the Goldstone-like mode of the SmAP$_F$ phase, based on the data of Fig. 2(a and b). The dashed curves are obtained by fitting eqn (1).

Results and discussion

The molecular structures and the phase sequence (refer to Fig. S3, ESI,† as a differential scanning calorimetry (DSC) chart) of the bent-shaped dimeric molecules 4OAM5AMO4 and 16OAM 5AMO16, and the mixture (4OAM5AMO4 (65 mol%) + 16O AM5AMO16 (35 mol%)) are given in Fig. 1.

To clarify both the non-collective and collective motions of the molecules, dielectric dispersion measurements were performed in the $SmCA^s$ (m = 4), SmC_AP_A (m = 16), and $SmAP_F$ (mixture of m = 4 and 16) phases. Here, it should be noted that the domain size is small especially in the $SmAP_F$ and the SmC_AP_A phases just as cooled from the isotropic phase. Hence, the domains of $SmAP_F$ and SmC_AP_A were enlarged by applying an AC field of 5 V_{pp} μm^{-1} and 33 V_{pp} μm^{-1}, respectively; they were grown by agitation of molecular motion due to ferroelectric switching. In Fig. 2(a) and (b), the real (ε') and imaginary (ε'') parts of the dielectric constants are plotted against the frequency from 10^1 to 10^7 Hz, respectively. Two relaxation modes are observed in this frequency range. One is a low frequency mode which is observed at approximately 500 Hz in the $SmAP_F$ phase and possesses huge dielectric constants. The low relaxation frequency (f_r) of the order of 1 kHz or less,[14–16] as well as the suppression under DC bias fields (mentioned later), shows that this mode is a Goldstone-like mode, collective fluctuation of polarization that is attributable to the ferroelectric phase. The other is a high frequency mode observed at approximately 100 kHz in the $SmCA^s$ and the SmC_AP_A phases. The isotropic phase also exhibits this mode. It is attributable to non-collective molecular rotation around the short axis of the mesogens as observed in conventional liquid crystal phases.[17,18]

Fig. 2(c) and (d) show the Cole–Cole plots for these two modes. The experimental dielectric spectra were further analyzed by fitting the following Cole–Cole model:[19]

$$\varepsilon^* = \varepsilon' - i\varepsilon'' = \varepsilon_\infty + \frac{\varepsilon_s - \varepsilon_\infty}{1 + (\omega\tau)^{1-\alpha}}$$

$$= \varepsilon_\infty + \frac{\Delta\varepsilon}{1 + (\omega\tau)^{1-\alpha}} \quad 0 < \alpha < 1, \qquad (1)$$

where ω is the angular frequency, ε_s and ε_∞ are the "static frequency" and "infinite frequency" dielectric constants, respectively, $\Delta\varepsilon$ is the dielectric strength, $\tau = 1/(2\pi f_r)$ is the relaxation time (where f_r is the relaxation frequency), and α is the distribution parameter of the relaxation time. For $\alpha = 0$ the Cole–Cole model reduces to the Debye model. The fitting according to the Cole–Cole equation is shown in Fig. 2(c and d) and Fig. 4(c), and the determined parameters are listed in Table S1. For the high-frequency relaxation of the $SmCA^s$ and the SmC_AP_A phases, α is around 1.0×10^{-3}. For the Goldstone-like mode of the $SmAP_F$ phase, on the other hand, α is between 0.04 and 0.14.

Most significant is that $\Delta\varepsilon$ is very large (approximately 1800) for the Goldstone-like mode of the $SmAP_F$ phase, whereas much smaller but usual values (<10) are observed in the high frequency mode of the $SmCA^s$ and the SmC_AP_A phases. A high

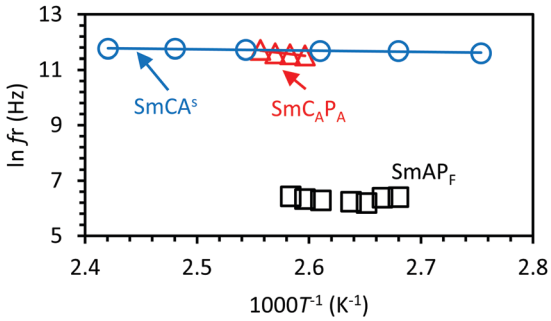

Fig. 3 Logarithm of the dielectric relaxation frequencies as a function of inverse absolute temperature for the $SmCA^s$, SmC_AP_A and $SmAP_F$ phases in a 3 μm-thick cell.

$\Delta\varepsilon$ has been reported in the ferroelectric phases of bent-shaped molecules.[14,20–22] W586 showed the maximum value of $\Delta\varepsilon$ (~300) as observed in a 3 μm-thick cell.[14] Furthermore, a bent-shaped azo molecule consisting of nonsymmetrical molecules with a lateral fluoro substitution on one of the wings achieved the maximum value of $\Delta\varepsilon$ (~400) in a 9 μm-thick cell.[22] The present $\Delta\varepsilon$ of 1800 exceeds these values substantially.

Fig. 3 shows the temperature dependence of the characteristic f_r of the relaxation processes observed in the $SmCA^s$, SmC_AP_A, and $SmAP_F$ phases in a 3 μm-thick cell. The high frequency mode observed in the $SmCA^s$ and SmC_AP_A phases follows the standard Arrhenius equation[20,22]

$$f_r = A \exp\left(-\frac{E_{act}}{k_B T}\right) \qquad (2)$$

where f_r is the relaxation frequency, A is the pre-exponential factor, E_{act} is the activation energy, k_B is the Boltzmann constant and T is the absolute temperature. Eqn (2) is fitted to the experimental data points in order to obtain E_{act}. The estimated E_{act} of the $SmCA^s$ and SmC_AP_A phases is 4 and 40 kJ mol^{-1}, respectively. In the higher temperature region, f_r of the $SmAP_F$ phase is somewhat temperature dependent, but seems to be independent in the lower temperature region as expected for the Goldstone mode.[23]

As another feature of the Goldstone-like mode of the $SmAP_F$ phase, f_r and $\Delta\varepsilon$ strongly depend on the cell thickness (refer to Fig. 4). As the thickness increases from 3 to 50 μm, f_r decreases from 500 to 300 Hz. On the other hand, $\Delta\varepsilon$ almost linearly grows; although $\Delta\varepsilon$ is approximately 1800 in a 3 μm-thick cell, it is 3200, 4500, and 7400 in 10, 25, and 50 μm-thick cells, respectively.

A similar thickness dependence of $\Delta\varepsilon$ for Goldstone-like modes has been observed in the ferroelectric chiral Sm-C*[24] and $SmAP_F$ phases.[14] Ozaki *et al.* found that some chiral Sm-C* materials possess dielectric constants larger than 7500 in a 250 μm-thick cell.[24] Guo *et al.* mentioned that by linear extrapolation of $\Delta\varepsilon$ for W586 an even larger value (~20 000) is expected for this cell thickness.[14] We estimated $\Delta\varepsilon$ by linear extrapolation similar to Guo *et al.* The expected $\Delta\varepsilon$ of 30 000 exceeds these values. One may speculate that such a cell

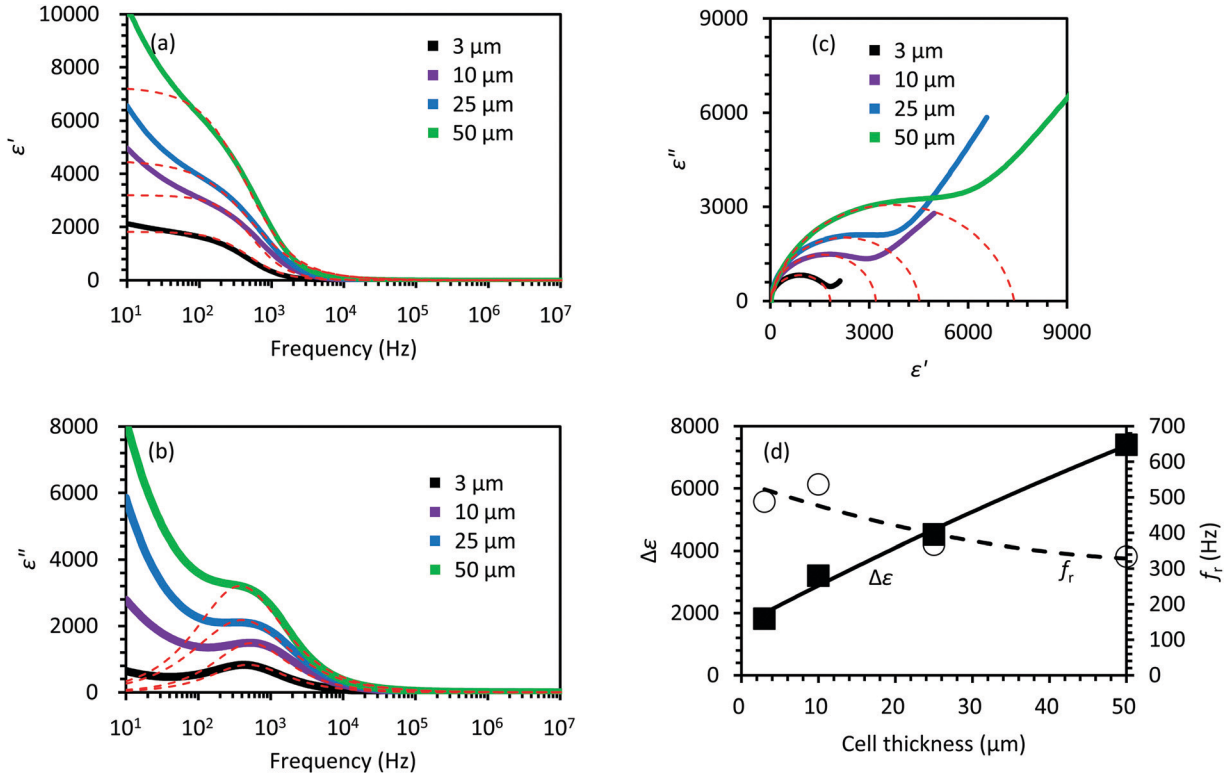

Fig. 4 (a) and (b) Frequency dependence of the real (ε') and imaginary (ε'') parts of the complex dielectric constants of the $SmAP_F$ phase in 3, 10, 25, and 50 μm-thick cells. The dashed curves are obtained by fitting eqn (1). (c) Cole–Cole plot of the $SmAP_F$ phase in 3, 10, 25, and 50 μm-thick cells. The dashed curves are obtained by fitting eqn (1). (d) Cell thickness dependence of $\Delta\varepsilon$ and the f_r in the $SmAP_F$ phase. The solid and dashed curves are guides for the eye.

thickness dependence is caused by strong anchoring of the molecules to the cell surfaces, which can prevent the collective fluctuations of dipoles near the cell surfaces. However, anchoring can cause significant suppression only in a thin cell, but not lead to a linear increase with the cell's thickness. A theoretical approach to explain this trend has been carried out by Guo *et al.*[14] They collected $\Delta\varepsilon$ with the cell where the bent direction of the bent-shaped molecules lay perpendicular to the cell's surface by strong surface anchoring. In such a cell, it is speculated that a splay of polarization arises across its thickness that can induce the cell thickness dependence in $\Delta\varepsilon$ and f_r in relation with the anchoring strength. Comparing the model and the experimental results, they have estimated the correlation length in the bulk and the surface to be approximately 10 and 1 μm, respectively.

In our case, however, the molecular orientation reported by Guo *et al.*[14] is unlikely. Fig. 5(a, c, and e) show the optical microscopic textures of the $SmAP_F$ phase in 3, 10, and 25 μm-thick cells, respectively. In all these cells, well-developed fan-shaped textures are observed, indicating the homogeneous alignment of the molecules, in other words, the alignment of the smectic layers perpendicular to the cell's surface. Fig. 5(b, d, and f) indicate the textures under DC bias fields. The textures do not change at all, but the birefringence colors change. This indicates that the bent (polar) direction of the molecules that are initially parallel to the cell's surface become perpendicular to it because of the ferroelectric response. On the

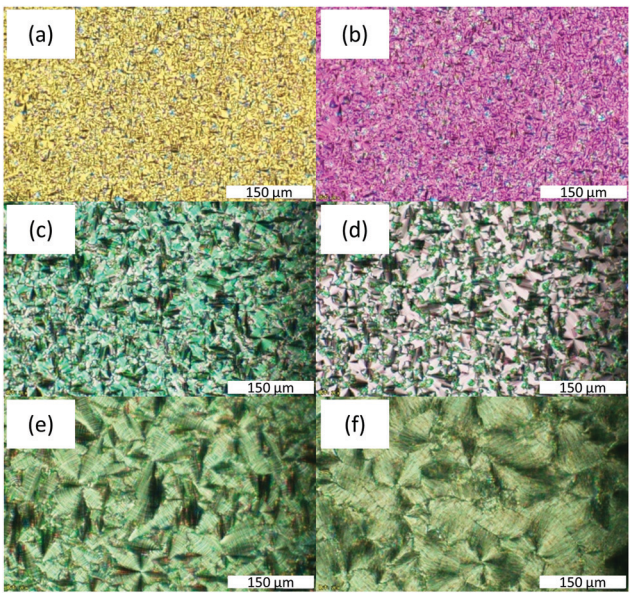

Fig. 5 Optical textures in the $SmAP_F$ phase (a) in a 3 μm-thick cell at 0 V μm^{-1}, (b) in a 3 μm-thick cell at 1 V μm^{-1}, (c) in a 10 μm-thick cell at 0 V μm^{-1}, (d) in a 10 μm-thick cell at 1 V μm^{-1}, (e) in a 25 μm-thick cell at 0 V μm^{-1} and (f) in a 25 μm-thick cell at 1 V μm^{-1}.

basis of the retardation obtained from the general polarization color chart, the birefringence (Δn) is estimated to be 0.07 at 0 V μm^{-1} and 0.18 at 1 V μm^{-1}, which are well expected from

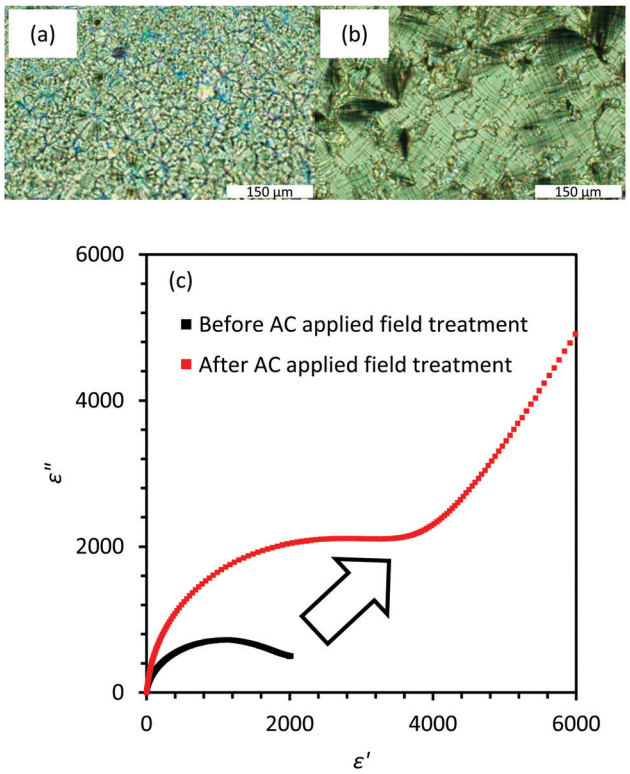

Fig. 6 Optical textures in the $SmAP_F$ phase in a 25 μm-thick cell (a) before application of an AC field and (b) after application of an AC field of 5 V_{pp} μm^{-1}. (c) Cole–Cole plot for the dielectric data of their $SmAP_F$ phases; $\Delta\varepsilon$ is 1900 and 4500 before and after AC application, respectively.

the parallelly and perpendicularly aligned models, respectively. In such a molecular alignment, the splay of polarization does not arise across the cell's thickness as reported by Guo *et al.*[14]

Fig. 5 shows the clear trend of the fan-shaped domain size increasing with the cell's thickness. Further, its average size roughly corresponds to the cell's thickness, meaning that the domain is uniform across the cell thickness. Thus, the coherence length of the molecular dipoles that cooperatively orient in the AC applied field increases with the increase of the cell's thickness. This increment, that is the increase of the number of molecules participating in the collective motion, may be responsible for the increase of $\Delta\varepsilon$ and the decrease of f_r.

The close relationship between the domain size and $\Delta\varepsilon$ can be seen even in the same cell. The domain size of the $SmAP_F$ phase as-cooled from the isotropic melt is fairly small and, as mentioned above, grows under AC applied fields. The estimated $\Delta\varepsilon$ in the former cell is very small. Examples, as observed in a 25 μm-thick cell, are shown in Fig. 6. $\Delta\varepsilon$ is 1900 while it becomes 4500 after the AC field treatment.

The relationship between the cooperative motion of dipoles and $\Delta\varepsilon$ has been treated theoretically[25] and experimentally.[26,27] Kirkwood[25] has extended Onsager theory by treating interacting dipoles, and has shown that $\Delta\varepsilon$ is proportional to

$$\frac{N\mu^2}{3kT}(1 + z\langle\cos\theta\rangle)$$

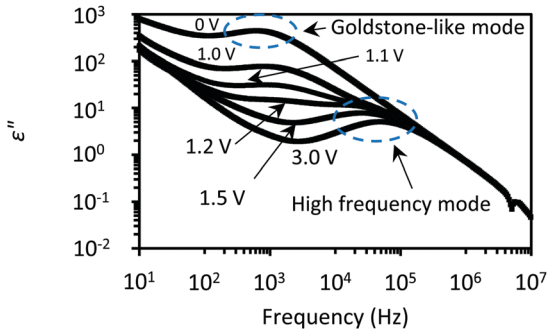

Fig. 7 The imaginary (ε'') part of the dielectric constants in the $SmAP_F$ phase measured under DC bias fields in a 3 μm-thick cell. Their values are presented on a log scale. The critical voltage is 1.2 V (0.40 V μm^{-1}) in a 3 μm-thick cell. The small depression observed at 6.0 × 10^6 Hz is the resonance effect due to the DC bias fields.[28]

where N is the number of dipoles per unit volume, μ is the dipole moment of the molecule, z is the coordination number (the number of interacting dipoles), and θ is the angle between the interacting dipoles. This was successfully applied for liquid water; its large dielectric constant of 80 is reproducible by $z = 4$ and $\langle\cos\theta\rangle = 0.5$. In a ferroelectric copolymer based on vinylidene cyanide, $z = 30$ and $\langle\cos\theta\rangle = 0.62$ were elucidated to explain the high dielectric constant of 130.[25] In analogy, we suppose that the huge $\Delta\varepsilon$ of the present molecular system may be attributable to the cooperative fluctuation of the large number of molecules $z = \sim 10^3$ which increases with the increase of the domain size.

The effect of DC bias fields on the Goldstone-like mode of the $SmAP_F$ phase was also studied. As shown in Fig. 7, by applying DC bias fields, the Goldstone-like mode is quickly quenched. As a result, the high frequency mode can be clearly detected at 100 kHz. The disappearance of the Goldstone-like mode is explained by the suppression of the dipoles' fluctuation due to the DC bias fields. Here, a cell thickness dependence is also observed in the critical voltage that suppresses the Goldstone-like mode. The critical voltage is 0.40 V μm^{-1} for a 3 μm-thick cell, 0.14 V μm^{-1} for a 10 μm-thick cell, and 0.06 V μm^{-1} for a 25 μm-thick cell (refer to Fig. S4, ESI†). This trend is the same as that reported by Guo *et al.*[14] but opposite to that reported by Shimbo *et al.*[29]

Conclusions

The dielectric relaxation properties were studied for the $SmAP_F$ phase in a bent-shaped dimeric molecule mixture of 4OAM5AMO4 (forming the $SmCA^s$ phase) and 16OAM5AMO16 (forming the SmC_AP_A phase). Within a cell of the $SmAP_F$ phase, the bent-shaped dimeric molecules lie with their bent plane parallel to the surface. The $SmAP_F$ phase shows a Goldstone-like mode at approximately 500 Hz characteristic of the ferroelectric phase and a huge $\Delta\varepsilon$ of over 7000 in a 50 μm-thick cell, which is much higher compared to almost all the reported values in bent-shaped molecules. The highly

cooperative orientation of the bent-shaped dimeric molecule is considered to bring about the giant value of $\Delta\varepsilon$. It is also characteristic of the Goldstone-like mode that the cooperative fluctuation of dipoles is easily quenched under DC bias fields. The extremely large value of the dielectric constants of the ferroelectric bent-shaped dimeric molecules suggests high potential for application in highly processible elements in electromechanical energy conversion devices.

Experimental

The mOAM5AMOm dimers with *m* values of 4 and 16 were synthesized following the methods reported in a previous report.[7] The bent-shaped dimeric molecule mixture of 4OAM5AMO4 (65 mol%) + 16OAM5AMO16 (35 mol%) was prepared by evaporating a chloroform solution of the two molecules at a predetermined molar ratio.[9] The phase transition temperatures were determined by DSC (SHIMADZU DSC-60 Plus) at a rate of 5 °C min^{-1} under cooling and heating runs. Texture observation and the identification of the mesophases were carried out using a polarizing optical microscope (OLYMPUS BX53) equipped with a hot stage and a temperature controller (Mettler Toledo FP 82HT). Electro-optical and dielectric investigations were performed using glass cells, having indium tin oxide (ITO) electrodes commercially available from EHC Co., Ltd. The area of the ITO electrodes was 100 mm^2, and the cell thicknesses of the ITO electrodes were 3, 10, 25, and 50 μm. In these cells, the bent-shaped dimeric molecules was homogeneously aligned with the bent plane parallel to the cell plane. Before the measurements, AC applied fields of 33 and 5 V_{pp} μm^{-1} were applied to 16OAM5AMO16 and 4OAM5AMO4 (65 mol%) + 16OAM5AMO16 (35 mol%) for the growth of liquid crystals, respectively. The complex dielectric constants were measured in the frequency range between 10^1 and 10^7 Hz with an impedance analyzer (FRA51615). The electric field was 1 V_{pp}.

Conflicts of interest

There are no conflicts to declare.

Acknowledgements

The authors would like to thank Professor Hiroshi Funakubo (Tokyo Institute of Technology) for valuable discussion on the dielectric properties. The authors would also like to thank Professor Masatoshi Tokita (Tokyo Institute of Technology) for usage of a triangular wave field device. The authors would also like to thank Professor Hideki Hosoda (Tokyo Institute of Technology) for usage of a differential scanning calorimetry tool. This work is supported by LG × JXTG Nippon Oil & Energy Smart Materials & Devices Collaborative Research Programs.

References

1 J. Watanabe, Y. Nakata and K. Shimizu, Frustrated bilayer smectic phase in main-chain polymers with two different spacers, *J. Phys. II*, 1994, **4**, 581–588.
2 T. Niori, T. Sekine, J. Watanabe, T. Furukawa and H. Takezoe, Distinct ferroelectric smectic liquid crystals consisting of banana shaped achiral molecules, *J. Mater. Chem.*, 1996, **6**, 1231–1233.
3 J. Watanabe, M. Hayashi, Y. Nakata, T. Niori and M. Tokita, Smectic liquid crystals in main-chain polymers, *Prog. Polym. Sci.*, 1997, **22**, 1053–1087.
4 G. Pelzl, S. Diele and W. Weissflog, Banana-Shaped Compounds-A New Field of Liquid Crystals, *Adv. Mater.*, 1999, **11**, 707–724.
5 H. Takezoe and Y. Takanishi, Bent-core liquid crystals: their mysterious and attractive world, *Jpn. J. Appl. Phys.*, 2006, **45**, 597–625.
6 J. Watanabe, T. Izumi, T. Niori, M. Zennyoji, Y. Takanishi and H. Takezoe, Smectic mesophase properties of dimeric compounds. 2. Distinct formation of smectic structures with antiferroelectric ordering and frustration, *Mol. Cryst. Liq. Cryst.*, 2000, **346**, 77–86.
7 T. Izumi, S. Kang, T. Niori, Y. Takanishi, H. Takezoe and J. Watanabe, Smectic mesophase behavior of dimeric compounds showing antiferroelectricity, frustration and chirality, *Jpn. J. Appl. Phys.*, 2006, **45**, 1506–1514.
8 T. Izumi, Y. Naitou, M. Tokita and J. Watanabe, Frustrated smectic phase appearing as transitional state between single-layer and antiferroelectric bilayer smectic phases in binary mixtures of dimeric compounds, *Jpn. J. Appl. Phys.*, 2006, **45**, 4991–4993.
9 T. Izumi, Y. Naitou, Y. Shimbo, Y. Takanishi, H. Takezoe and J. Watanabe, Several types of bilayer smectic liquid crystals with ferroelectric and antiferroelectric properties in binary mixture of dimeric compounds, *J. Phys. Chem. B*, 2006, **110**, 23911–23919.
10 J. Watanabe and S. Kinoshita, A distinct smectic C2 liquid crystal observed in main-chain liquid crystalline polymer, *J. Phys. II*, 1992, **2**, 1237–1245.
11 R. A. Reddy, C. Zhu, R. Shao, E. Korblova, T. Gong, Y. Shen, E. Garcia, M. A. Glaser, J. E. Maclennan, D. M. Walba and N. A. Clark, Spontaneous ferroelectric order in a bent-core smectic liquid crystal of fluid orthorhombic layers, *Science*, 2011, **332**, 72–77.
12 E. Gorecka, N. Vaupotic, and D. Pociecha, in *Handbook of Liquid Crystals*, ed. J. W. Goodby, P. J. Collings, T. Kato, C. Tschierske, H. F. Gleeson, and P. Raynes, Wiley-VCH Verlag GmbH & Co. KGaA., Germany, 2nd edn, 2014, vol. 13, pp. 1–33.
13 A. S. Tayi, A. Kaeser, M. Matsumoto, T. Aida and S. I. Stupp, Supramolecular ferroelectrics, *Nat. Chem.*, 2015, **7**, 281–294.
14 L. Guo, E. Gorecka, D. Pociecha, N. Vaupotič, M. Čepič, R. A. Reddy, K. Gornik, F. Araoka, N. A. Clark, D. M. Walba, K. Ishikawa and H. Takezoe, Ferroelectric behavior of orthogonal smectic phase made of bent-core molecules,

Phys. Rev. E: Stat., Nonlinear, Soft Matter Phys., 2011, **84**, 031706.

15 C. Filipič, T. Carlsson, A. Levstik, B. Žekš, R. Blinc, F. Gouda, S. T. Lagerwall and K. Skarp, Dielectric properties near the smectic-C*–smectic-A phase transition of some ferroelectric liquid-crystalline systems with a very large spontaneous polarization, *Phys. Rev. A: At., Mol., Opt. Phys.*, 1988, **38**, 5833–5839.

16 S. M. Khened, S. K. Prasad, B. Shivkumar and B. K. Sadashiva, Dielectric studies of Goldstone mode and soft mode in the vicinity of the A–C* transition, *J. Phys. II*, 1991, **1**, 171–180.

17 K. Hiraoka, H. Takezoe and A. Fukuda, Dielectric relaxation modes in the antiferroelectric smectic CA* phase, *Ferroelectrics*, 1993, **147**, 13–25.

18 J. Hatano, Y. Hanakai, H. Furue, H. Uehara, S. Saito and K. Murashiro, Phase sequence in smectic liquid crystals having fluorophenyl group in the core, *Jpn. J. Appl. Phys.*, 1994, **33**, 5498–5502.

19 K. S. Cole and R. H. Cole, Dispersion and absorption in dielectrics I, alternating current characteristics, *J. Chem. Phys.*, 1941, **9**, 341–351.

20 M. Marik, D. Jana, K. C. Majumder and B. K. Chaudhuri, Dielectric behavior in B1 and B2 phases composed of unsymmetrical bent shaped liquid crystal molecules, *Mol. Cryst. Liq. Cryst.*, 2015, **606**, 111–125.

21 S. A. Różański, Dielectric properties of liquid crystal formed by laterally fluorine-substituted banana-shaped molecules, *Phase Transitions*, 2018, **91**, 1007–1016.

22 J. Kumar and C. Prasad, Ferroelectric nematic and ferrielectric smectic mesophases in an achiral bent-core azo compound, *J. Phys. Chem. B*, 2018, **122**, 2998–3007.

23 M. R. Fuente, D. Dunmur, in *Handbook of Liquid Crystals*, ed. J. W. Goodby, P. J. Collings, T. Kato, C. Tschierske, H. F. Gleeson, and P. Raynes, Wiley-VCH Verlag GmbH & Co. KGaA., Germany, 2nd edn, 2014, 4, 1–46.

24 M. Ozaki, K. Yoshino, T. Sakurai, N. Mikami and R. Higuchi, Dielectric properties of new stable ferroelectric liquid crystals with large spontaneous polarization, *J. Chem. Phys.*, 1987, **86**, 3648–3654.

25 J. G. Kirkwood, The dielectric polarization of polar liquids, *J. Chem. Phys.*, 1939, **7**, 911–919.

26 T. Furukawa, Nonlinear dielectric and conductive spectra of polymers, *Makromol. Chem., Macromol. Symp.*, 1993, **70/71**, 183–192.

27 H. Ohigashi, K. Omote, H. Abe and K. Koga, Chain motions in the paraelectric phase in single crystalline films of vinylidene fluoride and trifluoroethylene copolymer P(VDF/TrFE), *J. Phys. Soc. Jpn.*, 1999, **68**, 1824–1827.

28 P. Perkowski, The parasitic effects in high-frequency dielectric spectroscopy of liquid crystals – the review, *Liq. Cryst.*, 2021, **48**, 767–793.

29 Y. Shimbo, E. Gorecka, D. Pociecha, F. Araoka, M. Goto, Y. Takanishi, K. Ishikawa, J. Mieczkowski, K. Gomola and H. Takezoe, Electric-Field-Induced Polar Biaxial Order in a Nontilted Smectic Phase of an Asymmetric Bent-Core Liquid Crystal, *Phys. Rev. Lett.*, 2006, **97**, 113901.